BMC Plant Biology

RESEARCH Open Access

Plastome phylogenomics unravels the evolutionary relationships and biogeographic history of Chloranthaceae

Peng-Wei Li[1], Yong-Bin Lu[1], Xin-Mei Qin[1] and Qiang Zhang[1*]

Abstract

Background Chloranthaceae is a pantropical family of flowering plants distributed mainly across Central and South America, East Asia, and the Pacific, encompassing approximately 73 species belonging to four extant genera—*Ascarina*, *Chloranthus*, *Hedyosmum*, and *Sarcandra*. As one of the most ancient lineages of extant angiosperms, Chloranthaceae holds substantial value in traditional medicine globally and offers major insights into the evolutionary history of flowering plants. However, phylogenetic relationships within this family remain partially resolved, and its origin continues to be debated. We here sequenced, assembled, annotated, and compared the chloroplast genomes (plastomes) of 22 Chloranthaceae species to investigate their plastome evolution and reconstructed the family's phylogeny by using both plastome and nuclear ribosomal DNA (nrDNA). Additionally, we employed the divergence-extinction-cladogenesis model to infer the ancestral area and historical migration patterns of Chloranthaceae.

Results Results The plastomes of Chloranthaceae exhibit a typical quadripartite structure, with genome sizes ranging from 157,449 bp to 159,218 bp and encoding 113 unique genes, including 17–18 genes duplicated in inverted repeat (IR) regions. Interestingly, the genus *Hedyosmum* demonstrated notable IR expansions, resulting in $trnH^{GUG}$ duplication in five species. A comparative analysis unveiled substantial variations in simple sequence repeats (SSRs) and tandem repeats across different species, whereas interspersed repeats remained relatively stable. Correlation analyses revealed positive correlations between plastome size and both IR length and SSR count. Furthermore, our phylogenetic reconstruction based on plastome and nrDNA (18 S-ITS1-5.8 S-ITS2-26 S) data provided robust support for the intergeneric relationships, confirming the monophyly of each genus and resolving long-standing uncertainties in the intrageneric relationships of *Chloranthus* and *Hedyosmum*. Notably, *H. orientale*, the sole *Hedyosmum* species found in Asia, was phylogenetically embedded within the genus, rather than occupying a basal position contrary to previous results. Our biogeographical reconstruction, incorporating both extant and fossil evidence, supports a Laurasian origin of Chloranthaceae and its subsequent dispersal to the tropics.

Conclusion Conclusions This study provides the most comprehensive plastome-based phylogenomic analysis of Chloranthaceae to date, offering novel insights into its plastome evolution, resolving long-standing ambiguities in interspecific and phylogenetic relationships and reconstructing the probable biogeographic origin and historical

*Correspondence:
Qiang Zhang
qiangzhang04@126.com

Full list of author information is available at the end of the article

migrations of this family. The proposed resources establish a robust framework for future evolutionary investigations within the realm of Chloranthaceae.

Keywords Biogeography, IR expansion, Laurasian, Phylogeny, Plastome, Repeat sequence

Introduction

Chloranthaceae is a small pantropical family of flowering plants primarily distributed across tropical and subtropical regions of South America, East Asia, and the Pacific [1]. As one of the most ancient lineages of extant angiosperms and given its basal phylogenetic position among angiosperms, along with a rich fossil record traceable to the Early Cretaceous, Chloranthaceae serves as a vital resource that provides insights into the origin and early diversification of flowering plants [1–3]. According to the International Plant Names Index (https://www.ipni.org/), the family comprises approximately 73 species belonging to four extant genera, namely *Ascarina* J.R.Forst. & G.Forst.(12 species), *Chloranthus* Sw.(14 species), *Hedyosmum* Sw. (45 species), and *Sarcandra* Gardner (2 species). Chloranthaceae plants typically inhabit shaded and moist environments, surviving as understory shrubs or small trees [1]. The family is known for its morphologically reduced fertile parts (flowers), possessing a single stamen and/or a single carpel with a pendent orthotropous ovule, which has long intrigued morphologists and paleobotanists [4–12]. In addition to their evolutionary importance, Chloranthaceae species have significant medicinal value and are widely used in ethnomedical practices and traditional medicines in various regions across Asia, South America, and Central America. Different species within this family have been traditionally used as antispasmodic, antiseptic, and anticancer drugs, as well as for relieving aches, boils, and dermatopathia [13–18]. Various biologically active compounds have been isolated from different Chloranthaceae species, including terpenoids, flavonoids, coumarins, organic acids, and sterols, underscoring their potential pharmaceutical importance [13]. Therefore, the dual significance of Chloranthaceae—in evolutionary biology and traditional medicine and ethanomedicine worldwide—has made it a subject of interest and scientific investigations.

For more than 30 years, molecular data have played a pivotal role in resolving the phylogenetic relationships within angiosperms [19]. Contemporary molecular phylogenies position Amborellales, Nymphaeales, and Austrobaileyales as successive sisters to Mesangiospermae, which can be further categorized into five major clades: eudicots, monocots, magnoliids, Chloranthales, and Ceratophyllales [20, 21]. Among these, Chloranthales has been consistently placed as the sister group to magnoliids in several recent phylogenetic studies [19, 22, 23]. However, alternative topologies have also been proposed, resulting ongoing debates regarding the exact placement of Chloranthales within the angiosperm phylogeny [24–26]. As the sole family within Chloranthales, Chloranthaceae has attracted considerable research attention for its evolutionary significance as mentioned above. Phylogenetic investigations within Chloranthaceae date back to the late 20th century. Qiu et al. [2] explored the intrafamilial relationships of the family by using four sampled species and five molecular markers from the mitochondrial, plastid, and nuclear genomes. Their findings unveiled a close relationship between *Chloranthus* and *Sarcandra*, with *Ascarina* and *Hedyosmum* successively diverging from these two genera. This relationship was subsequently confirmed by Qiu et al. [27] and Zanis et al. [28] who used similar taxon sampling. Subsequent phylogenetic analyses by Kong et al. [8] focused on *Chloranthus*, employing ITS and *trnL-F* markers to investigate the evolutionary origin of the tripartite androecium within this genus. Zhang and Renner [29] were the first to examine both infrafamilial and infrageneric relationships in 20 Chloranthaceae species through phylogenetic analyses with four chloroplast sequence segments. Their study provided strong support for consistent intergeneric relationships; however, the interspecies phylogenetic relationships within the same genus remained unresolved. Using ITS and two chloroplast regions, Antonelli and Sanmartín [30] expanded the scope of research to 42 Chloranthaceae species, specifically focusing on *Hedyosmum*. They constructed a comprehensive phylogenetic framework of those species. Zhang et al. [9] revisited Chloranthaceae phylogeny by using a combined dataset of three plastid DNA regions and 56 species, contributing insights into the family's temporal evolutionary history. However, significant phylogenetic incongruence between the plastid and nuclear phylogenies in Chloranthaceae was subsequently revealed by Zhang et al. [10]. They highlighted how this conflict affects our understanding of organismal relationships, biogeographical history, morphological evolution, and phylogenetic diversity. Despite extensive phylogenetic studies, systematic phylogenomic investigations are lacking for Chloranthaceae. Currently, only seven complete plastomes and two nuclear genomes are available for the family [19, 23, 31–38]. However, the lack of high-quality phylogenomic data and broad taxon sampling has prevented the resolution of infrageneric relationships, highlighting the critical need for conducting plastome phylogenomic analyses to establish definitive frameworks.

In addition to the unresolved phylogenetic relationships, the biogeographic origin of Chloranthaceae has

been a subject of considerable debate. Based on the modern distribution of the four extant genera, Raven and Axelrod [39] proposed a Laurasian origin, suggesting that the genus *Hedyosmum*—currently dominant in tropical America, likely diverged in Laurasia before dispersing to North America and subsequently colonizing South America. By contrast, Krutzsch [40], based on fossil distributions, advocated for a West African and northwestern Gondwanan origin. Zhou [41], utilizing fossil evidence, argued for a southeastern Laurasian origin, particularly along the eastern margins of the Paleo-Northern continent (Laurasia), specifically within the Malaysian phytogeographic region. Zhou's hypothesis posits that *Hedyosmum* likely originated in this region, subsequently dispersing westward into North America and migrating southward toward Central America. Chen and Cheng [42] challenged this hypothesis by presenting paleoenvironmental evidence supporting that the Malay Archipelago and adjacent regions did not emerge as stable subaerial landmasses until Late Cretaceous, rendering them unlikely centers of origin for Chloranthaceae. Instead, Chen and Cheng promoted a peri-North Atlantic origin, encompassing both northwestern Gondwana and southwestern Laurasia during Late Cretaceous. Several new Chloranthaceae fossils from Cretaceous strata have recently been discovered [43], substantially expanding the available paleobotanical evidence for the family's early diversification. Despite accumulating fossil records, paleontological evidence remains to be integrated with extant biogeographic data of Chloranthaceae for a comprehensive analysis of its origin.

Given the unresolved phylogenetic relationships and ongoing debate regarding the origin of Chloranthaceae, the present study addressed the following objectives: (1) characterize the plastome features of Chloranthaceae species, (2) reconstruct the phylogenetic relationships within the family using genome skimming data; and (3) infer the geographic origin of Chloranthaceae by integrating molecular phylogenies with fossil evidence. Based on the results, we established a robust phylogenomic framework for Chloranthaceae, providing further insights into the evolutionary processes and phylogenetic connections within the basal angiosperm Chloranthaceae. Additionally, the data obtained will serve as a valuable genetic resource for future research on molecular marker development, molecular breeding, and other investigations related to Chloranthaceae.

Materials and methods

Taxon sampling, DNA extraction, and sequencing

We sampled 22 Chloranthaceae species, representing all sections across the four genera within the family [9, 30, 44], including two *Ascarina* species, 11 *Chloranthus* species, eight *Hedyosmum* species, and one *Sarcandra* species (see Table S1 for details). Healthy, clean, and mature leaves were collected, dried in silica gel, and stored for subsequent DNA extraction. Total genomic DNA was extracted from dry leaves by using a modified cetyltrimethylammonium bromide (CTAB) method [45]. The quality and quantity of the extracted DNA were assessed through 1.0% agarose gel electrophoresis and by using a Nanodrop™ 2000 spectrophotometer (Thermo Fisher Scientific, USA). Genomic DNA libraries were constructed with an insert size of 200–500 bp and Illumina paired-end read length of 150 bp, followed by sequencing on an Illumina HiSeq 2500 platform at Biomarker Technologies Inc., Beijing, China. A minimum of 3 Gb raw sequencing data were obtained for each species.

Plastome assembly and annotation

Raw sequencing reads were trimmed to remove adapter sequences and low-quality bases by using Trimmomatric v.0.36 [46]. The quality of the filtered reads was assessed using FastQC (http://www.bioinformatics.babra-ham.ac.uk/projects/fastqc), ensuring a PHRED quality score of >30. De novo plastome assembly was performed using GetOrganelle v.1.7.7, with default parameter settings [47]. For *Sarcandra glabra*, GetOrganelle failed to generate a complete plastome assembly; therefore, the raw reads were mapped to non-overlapping scaffolds in Geneious v.7.1.8, extending the ends of the scaffolds to close gaps through iterative mapping with medium-to-low sensitivity (100 iterations) [48].

Plastomes were annotated using the plastid genome annotator [49], using *Amborella trichopoda* (Accession No. AJ506156) and *Chloranthus spicatus* (Accession No. EF380352) as reference plastid genome sequences. tRNA genes were further verified using tRNAscan-SE [50]. The boundaries of the start and stop codons and the exon-intron boundaries were carefully inspected manually and curated in Geneious v. 7.1.8, with the published Chloranthaceae plastomes as references [48]. The general characteristics of the plastomes, including total sequence length, GC content, and gene content, were also obtained using Geneious v. 7.1.8. Circular plastome maps were visualized using OGDRAW v.1.3.1 [51].

Comparative plastome analyses for 22 Chloranthaceae species

To investigate variations in the size and number of genes in the plastomes, likely caused by the expansion or contraction of the IR region, boundaries between the IR and single-copy regions were examined manually in Geneious v. 7.1.8, and a schematic was manually created to visualize structural variations [48].

To avoid redundancy, repeat sequence analysis was performed in the 22 Chloranthaceae plastomes with one inverted repeat (IR) region removed. Three classes of

repeats were identified: microsatellites, also known as simple sequence repeats (SSRs); dispersed repeats; and tandem repeats. SSRs were detected using MISA-web [52], with a minimum threshold of 10, 5, 4, 3, 3, and 3 repeat units for mono-, di-, tri-, tetra-, penta-, and hexanucleotide motifs, respectively. Two SSRs located next to each other without any space were together considered a compound SSR. Dispersed repetitive sequences, including forward (F), reverse (R), complementary (C), and palindromic (P) repeats, were identified using the REPuter web server [53], with the minimum repeat size of 30 bp, a sequence identity of ≥ 90%, a Hamming distance of 3, and a minimum repeat size of ≥ 30 bp. Furthermore, tandem repeats (≥ 10 bp) were detected using Tandem Repeats Finder [54] with alignment parameters set as follows: match = 2, mismatch = 7, InDel = 7, a minimum alignment score of 50, and a maximum period size of 500. All identified repeats were manually verified to eliminate redundancy. Correlations between the plastome size, number of different types of repeats (SSRs, dispersed repeats and tandem repeats), and the IR region length were analyzed using R v. 4.3.1 [55].

Phylogenetic analysis

Phylogenetic relationships were reconstructed using both plastomes and nuclear ribosomal DNA (nrDNA, including 18 S-ITS1-5.8 S-ITS2-26 S) from 22 Chloranthaceae species (Table S1). Two magnolia species, *Beilschmiedia yunnanensis* Hu and *Liriodendron chinense* (Hemsl.) Sargent., were included as outgroups based on recent phylogenomic studies [22, 23]. Maximum likelihood (ML) and Bayesian inference (BI) methods were used for phylogenetic analyses. All analyses were conducted using the CIPRES Science Gateway [56]. ModelFinder [57] in IQ-TREE v. 1.7 [58] was used to identify the best-fit partition scheme and nucleotide substitution models for both the plastid supermatrix and nrDNA dataset. To assess uncertainty in the topology, ML analysis was performed in RAxML v. 8.2.12 [59], with the GTRGAMMA model and 1000 rapid bootstrap (BS) inferences by using the best partition scheme suggested by ModelFinder. The BI analysis was conducted in MrBayes v. 3.2.7 [60] using the best partition scheme and ModelFinder-derived model. Ten million generations were run in two independent analyses, each with four Markov chain Monte Carlo chains. Trees were sampled every 1000 generations (= 10,000 trees) and the first 25% of the trees were discarded as burn-in. The remaining trees were used to generate a 50% majority-rule consensus tree. Convergence was assessed by ensuring split frequencies with an average standard deviation of < 0.01.

Ancestral area reconstruction

To infer the biogeographic origin of Chloranthaceae, we performed ancestral area reconstructions by integrating extant species distribution data and fossil records. Chloranthaceae species are primarily distributed across three major regions: Central and South America, East Asia and Indomalaysia, and the South Pacific Islands. However, recent discoveries have provided evidence supporting the existence of Chloranthaceae macro- and meso-fossils across broader geographic ranges, including North America, Europe, and Antarctica [43]. Therefore, we conducted ancestral area reconstruction by using either the data of extant Chloranthaceae species distribution alone or in combination with their fossil records. Integrating the extant distribution of Chloranthaceae with paleocontinental dynamics, five biogeographic units were established for extant taxa: (a) Central America, (b) South America, (c) East Asia, (d) Indian subcontinent, and (e) South Pacific Islands. Although *Ascarina* is distributed in Madagascar, phylogeographic evidence supports its origin through secondary transoceanic dispersal from the South Pacific [10, 39]. Therefore, based on its exclusion from our sampling and secondary dispersal origin, we excluded Madagascar from the biogeographic delineation. When incorporating fossil data, the extant biogeographic framework was augmented by adding three more regions: (f) Antarctic Peninsula, (g) eastern North America, and (h) western Europe. To minimize phylogenetic uncertainty, fossil taxa with clearly established phylogenetic placement within crown Chloranthaceae were incorporated. Fossil pollen types, such as the widely distributed *Asteropollis* [61] were excluded from our study because of their ambiguous taxonomic affinity [43]. The six biogeographic models, namely the divergence-extinction-cladogenesis (DEC), DIVALIKE, BAYAREALIKE frameworks and their respective + j variants, which incorporate founder-event speciation, were tested using BioGeoBEARS [62] implemented in the RASP 4.2 platform [63]. Ancestral area reconstructions were performed using BioGeoBEARS. The phylogenetic tree of extant Chloranthaceae was derived from present study (see Results), while the comprehensive tree for all Chloranthaceae taxa (including fossils) was based on Friis et al.'s framework [43]. The respective outgroups from both trees were removed to minimize topological biases, and the trees were employed as independent inputs for ancestral range reconstruction.

Results

Plastome features of Chloranthaceae

Following quality control and preprocessing, a minimum of three gigabases of whole-genome sequencing data were obtained for each of the 22 Chloranthaceae species. The clean reads were assembled into high-quality plastomes

by using de novo assembly methods. The resulting average base-coverage varied from 54 × in *Hedyosmum maximum* and *H. goudotianum* to 535 × in *Sarcandra glabra* (Table 1). All newly assembled plastomes exhibit a typical quadripartite structure, comprising a large single copy (LSC) region, a small single copy (SSC) region, and a pair of inverted repeat (IR) regions (Fig. 1).

The overall structure of the Chloranthaceae plastomes is largely conserved across the family (Table 1). The plastome size ranges from 157,449 bp (*C. fortunei*) to 159,218 bp (*H. brenesii*). Notably, most *Chloranthus* species (< 15.8 kb) have shorter plastomes than *Ascarina*, *Sarcandra*, and most *Hedyosmum* species (> 15.8 kb). The SSC region in *Hedyosmum* species is slightly shorter than that in *Ascarina*, *Sarcandra*, and *Chloranthus* species. However, the IR region in *Hedyosmum* species was found to be the longest among the four genera (Table 1). The overall GC content is almost consistent among the genera, ranging from 38.8 to 39.2%. However, it exhibits regional differences, with the LSC region ranging from 37.3 to 37.8%, the SSC region from 33.8 to 34.6%, and the IR region from 43.1 to 43.4%. In addition, the total number of annotated genes per plastome ranges from 130 to 131, comprising 85 protein-coding genes and eight rRNA genes. The variation in gene numbers is primarily attributed to the number of tRNA genes, which ranges from 37 to 38 (Table 1).

Each Chloranthaceae plastome was found to contain 113 unique genes, including 79 protein coding genes, 30 tRNA genes, and four rRNA genes. Among them, 16 genes contain a single intron, while two genes (*clpP* and *ycf3*) contain two introns each. Additionally, 16 or 17 genes are completely duplicated within the IR regions (Table S2). The *rps12* gene is partially duplicated, a common feature in most angiosperm plastomes. In the 22 Chloranthaceae plastomes, *rps12* functions as a trans-splicing gene, with its 5'-end exon located in the LSC region and the intron and 3'-end exon situated in the IR region. The $trnH^{GUG}$ gene has undergone duplication in *H. bonplandianum*, *H. goudotianum*, *H. orientale*, *H. nutans* and *H. brenesii* (Fig. 1, Table S2).

Contraction and expansion of IR regions

Figure 2 provides a comparative account of IR/SC boundary contents across the 22 Chloranthaceae plastomes. We found that the overall genomic structure, including the gene number and order, is well-conserved among the species. However, differences were observed in the IR/SC boundary regions. Specifically, in the five *Hedyosmum* species (namely *H. bonplandianum*, *H. goudotianum*, *H. orientale*, *H. nutans* and *H. brenesii*), the $trnH^{GUG}$ gene is positioned in the IR region and separated from the IRB/LSC or IRA/LSC boundary by 90–155-bp spacers. Nonetheless, in *C. angustifolius*, the $trnH^{GUG}$ gene is entirely located in the LSC region and separated from the IRA/LSC boundary by a 12 bp spacer. By contrast, in the remaining 16 Chloranthaceae species, the $trnH^{GUG}$ gene crosses the IRA/LSC boundary, leaving a 10–20 bp pseudogene copy $\psi trnH^{GUG}$ at the IRB/LSC junction without any spacer. The *ycf1* gene spans the IRB/SSC boundary in all species, whereas the pseudogene *ψycf1* at the IRA/SSC boundary varies in size from 1303 bp to 1416 bp. The *ndhF* gene overlaps with the *ψycf1* gene, sharing 5–27 nucleotides, or the two genes are separated by 6–77-bp spacers. Notably, in the five *Hedyosmum* species, the IR regions extend to the SC regions, whereas in the remaining species, these regions show contraction. Moreover, the IR/SC boundary structure was found to be shared within two groups of *Chloranthus* species, with *C. serratus*, *C. henryi* and *C. oldhamii* forming one group, and *C. fortunei* and *C. coccineus* forming another. This shared boundary pattern is suggestive of a close phylogenetic relationship among the species.

Repeat sequence analyses

In total, 1296 SSRs were identified in the 22 Chloranthaceae plastomes through the MISA analysis (Fig. 3). The number of SSRs ranges from 40 in *C. fortunei* to 88 in *H. nutans*. The *Hedyosmum* species exhibit a higher SSR count (Fig. 3A–C). Additionally, the distribution of SSRs is uneven throughout the plastomes, with a notable absence of SSRs in the IR regions of some *Chloranthus* species (Fig. 3B). Most SSRs were detected in the intergenic spacers, with the number ranging from 62.96% in *A. swamyana* to 79.59% in C. *erectus* (Fig. 3A, Table S3). The LSC region contained the majority of SSRs, ranging from 64.86% in *H. brenesii* to 86.00% in *C. nervosus* (Fig. 3B). Mononucleotide repeats were the most prevalent, constituting 61.96% of all SSRs, followed by dinucleotide (14.89%) and tetranucleotide (10.65%) repeats (Fig. 3C, Table S3). Pentanucleotide and hexanucleotide repeats were rare in some Chloranthaceae species, collectively accounting for only 2.47% and 1.7% of the total SSRs, respectively. The distribution of different SSR types slightly varied among the four genera of Chloranthaceae. The average percentage of mononucleotide SSRs was higher in *Hedyosmum* than in the other three genera. By contrast, the average percentage of di-, tri-, tetra-, penta-, and hexanucleotide SSRs was mostly lower in *Hedyosmum* than in the other three genera. In addition, a strong A/T bias was observed in the base composition of mono- and dinucleotide SSRs: A/T and AT/TA being the most abundant for mononucleotide and dinucleotide repeats, respectively (Fig. 3D and Table S4). Additionally, several genus-specific SSRs were detected. Three SSRs (CATA/TACT/TTTC) were unique to *Chloranthus* and *Sacandra*, six SSRs (CT, AAG, CAA, AATGAT, ATACAA, and CTTACA) were found only in *Ascarina*, and three SSRs

Table 1 Basic characteristics of the plastomes generated in this study

Species	Total length (bp)	LSC (bp)	SSC (bp)	IR (bp)	Gene count	PCG count	rRNA count	tRNA count	GC content (%)	GC content in LSC (%)	GC content in SSC (%)	GC content in IR (%)	Average base-cover-age
Ascarina rubricaulis	158,415	87,446	18,675	26,147	130	85	8	37	39.0	37.7	33.8	43.2	491
A. swamyana	158,381	87,367	18,696	26,159	130	85	8	37	39.1	37.7	33.9	43.2	249
Chloranthus angustifolius	157,566	86,734	18,542	26,145	130	85	8	37	38.9	37.4	34.1	43.2	443
C. coccineus	157,475	86,582	18,499	26,197	130	85	8	37	38.9	37.4	34.0	43.1	466
C. erectus	157,735	87,055	18,410	26,135	130	85	8	37	38.9	37.4	33.9	43.2	526
C. fortunei	157,449	86,647	18,502	26,150	130	85	8	37	38.9	37.4	34.1	43.2	430
C. henryi	157,957	87,127	18,528	26,151	130	85	8	37	38.9	37.3	34.0	43.2	361
C. japonicus	158,639	87,720	18,627	26,146	130	85	8	37	38.8	37.3	33.9	43.2	249
C. nervosus	158,510	87,626	18,524	26,180	130	85	8	37	38.9	37.3	34.1	43.1	527
C. oldhamii	157,705	86,915	18,484	26,153	130	85	8	37	38.9	37.4	34.0	43.2	217
C. serratus	157,893	87,039	18,550	26,152	130	85	8	37	38.9	37.3	34.0	43.2	490
C. sessilifolius	157,614	86,860	18,490	26,132	130	85	8	37	38.9	37.4	34.0	43.2	375
C. spicatus	157,781	87,040	18,455	26,143	130	85	8	37	38.8	37.3	33.9	43.1	280
Hedyosmum bonplandianum	158,297	87,340	18,067	26,445	131	85	8	38	39.0	37.5	34.0	43.3	55
H. brenesii	159,218	87,956	18,246	26,508	131	85	8	38	39.0	37.5	33.9	43.3	145
H. goudotianum	158,198	87,293	18,067	26,419	131	85	8	38	39.0	37.5	33.9	43.3	55
H. maximum	158,075	87,856	17,777	26,221	130	85	8	37	39.0	37.4	34.0	43.3	54
H. mexicanum	157,557	87,324	17,763	26,235	130	85	8	37	39.0	37.4	33.9	43.4	138
H. nutans	159,027	87,921	18,218	26,444	131	85	8	38	39.0	37.5	34.0	43.3	290
H. orientale	158,015	87,117	18,208	26,345	131	85	8	38	39.1	37.6	34.0	43.4	137
H. peruvianum	158,082	87,870	17,778	26,217	130	85	8	37	39.0	37.3	34.0	43.4	90
Sarcandra glabra	158,902	88,192	18,444	26,133	130	85	8	37	39.2	37.8	34.6	43.3	535

Note: PCG, protein-coding genes

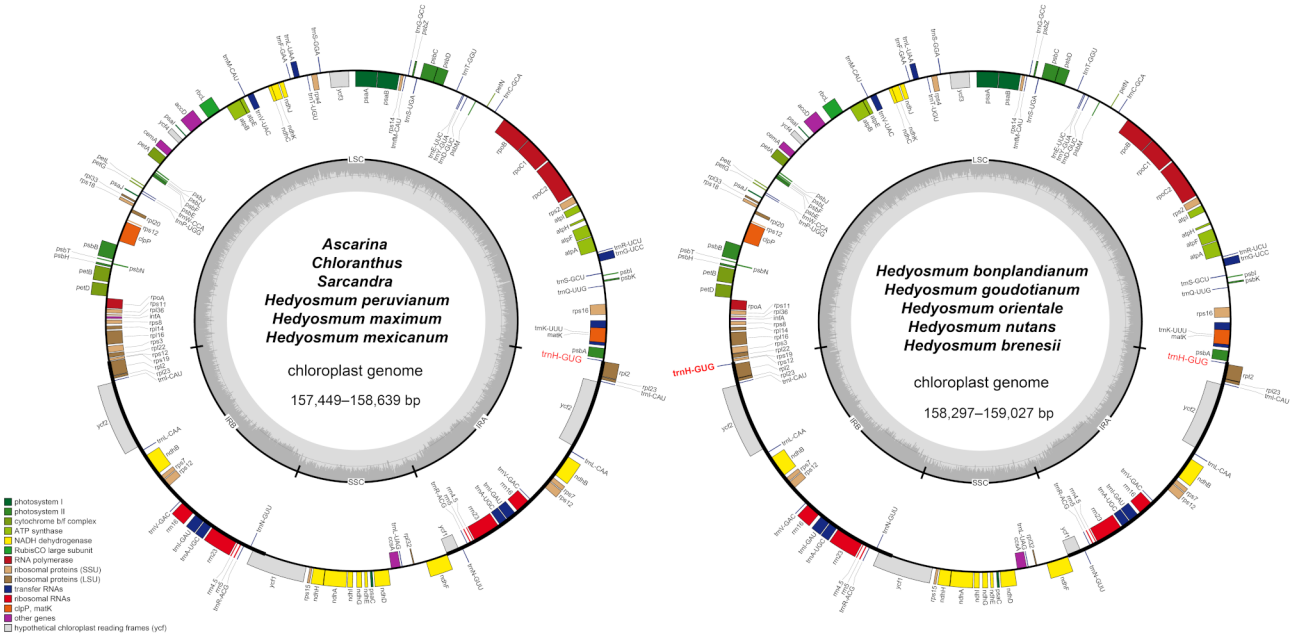

Fig. 1 Circular gene map of the plastid genome of Chloranthaceae species. Genes facing inside and outside of the outer circle are transcribed in the clockwise and counterclockwise directions, respectively. Genes belonging to different functional groups are color coded. Dark gray bars in the inner circle indicate the GC content. Red font indicates the difference between the two gene maps

(AC/TC/CCCT) were exclusive to *Hedyosmum* (Fig. 3D, Table S4).

Using REPuter, we identified 445 dispersed repeats in the 22 Chloranthaceae plastomes, comprising 275 forward, 140 palindromic, 17 reverse, and 13 complement repeats (Table S5). Complement repeats were not detected in *Ascarina* and *Hedyosmum* (Fig. S1A and, Table S5). The number of dispersed repeats ranged from 13 in *C. sessilifolius* to 27 in *C. angustifolius*. The length of those repeats varied from 30 to 97 bp (Table S6). Most of the repeats were shorter than 40 bp, with only two species (*S. glabra* and *H. brenesii*) having repeat length exceeding 90 bp (Fig. S1B, Table S5–6). Tandem Repeats Finder detected a total of 286 tandem repeats, with the majority found in the intergenic spacers (Fig. S1C). The number of tandem repeats in *Chloranthus* species ranged from 11 in *C. sessilifolius* to 30 in *C. japonicus* while the other three genera generally had fewer than 10 tandem repeats (Fig. S1C, D and Table S7–8). These results indicated that the number of tandem repeats is lineage specific and their length is mostly less than 20 bp (Fig. S1C, D).

Plastome size in Chloranthaceae positively correlated with both IR length ($R = 0.5$, $p = 0.017$) and SSR number ($R = 0.48$, $p = 0.023$) (Fig. 4). It correlated positively with the number of dispersed repeats ($R = 0.38$, $p = 0.084$) but negatively and non-significantly with the number of tandem repeats (R = -0.065, $p = 0.78$) (Fig. S2). The increase in plastome size is likely attributable in part to the expansion of IR regions and the presence of SSRs, which are primarily located in the intergenic spacer and the LSC region (Fig. 3A–B).

Phylogenetic relationships of Chloranthaceae

The plastome matrix had a total alignment length of 137,387 bp (with one IR removed), with 14,218 sites being parsimony-informative. The nrDNA contained 6,004 bp, of which 491 sites were parsimony-informative. The ModelFinder analysis recommended partitioning the plastome into 14 parts, with the best-fit model being HKY for one partition and GTR for the others (Table S9). The best-fit model for nrDNA was GTR.

Both ML and BI trees constructed from the plastome matrix exhibited identical topologies, with strong support across all nodes (Fig. 5A). Within *Chloranthus*, two major clades were identified, with one containing six species and the other containing five species. The first clade contained *C. sessilifolius* and *C. oldhamii* as sister species, both of which grouped with *C. serratus* and *C. henryi* with strong support. Another pair of sister species, *C. erectus* and *C. spicatus*, clustered together with the first four species with maximum support. The second clade comprised five species. *Chloranthus coccineus* and *C. fortunei*, both clustering with *C. angustifolius* with strong support. *Chloranthus nervosus* and *C. japonicus* formed a sister pair, clustering with the aforementioned three species with maximum support. Two distinct clades were also identified with *Hedyosmum* (Fig. 5A). The first clade included *H. peruvianum* and *H. maximum* as sister species, followed by *H. mexicanum*, and another sister pair,

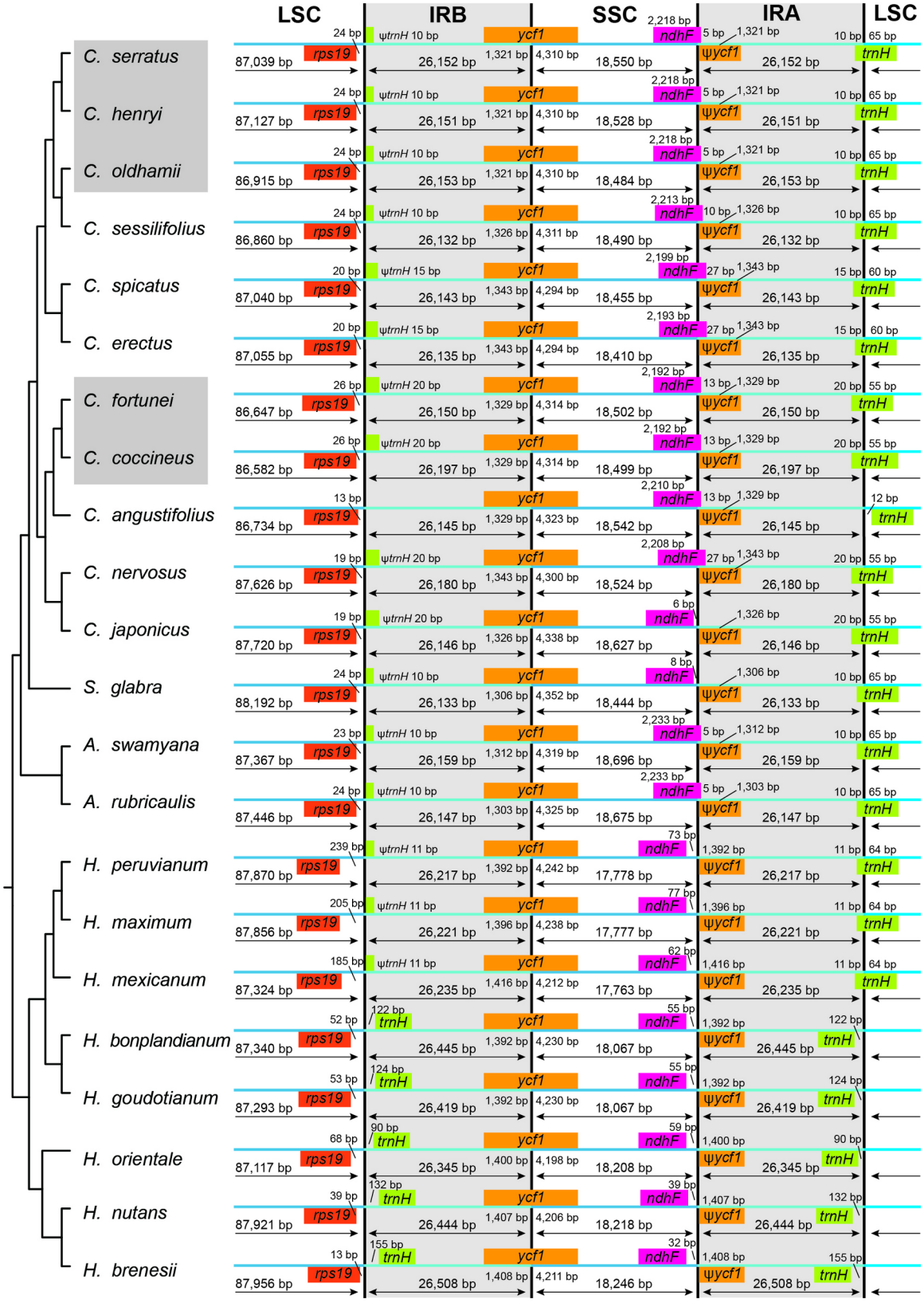

Fig. 2 Comparison of LSC, IR, and SSC border regions among the 22 Chloranthaceae plastid genomes. Genes above and below the line are transcribed from right to left and left to right, respectively. Lengths of genes and regions are not drawn to scale. Using Bayesian method, the cladogram on the left is generated based on plastomes, and the shadowed species share identical border regions of the plastid genome. Ψ indicates a pseudogene

Fig. 3 Analysis of simple sequence repeats (SSRs) for the 22 Chloranthaceae plastid genomes. (**A**) Number of SSR in the coding regions (CDS), intergenic regions (IGS), and introns. (**B**) Number of SSR in LSC, SSC, and IR regions. (**C**) Type of SSR among the 22 Chloranthaceae plastomes. (**D**) Type and number of SSRs in different Chloranthaceae species

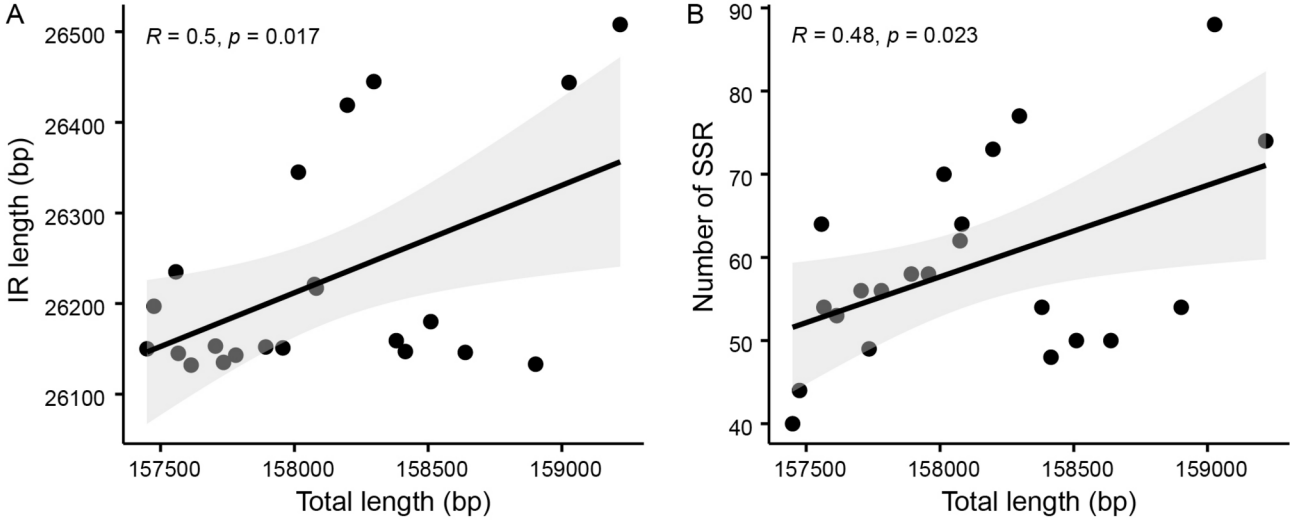

Fig. 4 Analyses for the correlation of plastome length with IR length (**A**) and number of SSR (**B**)

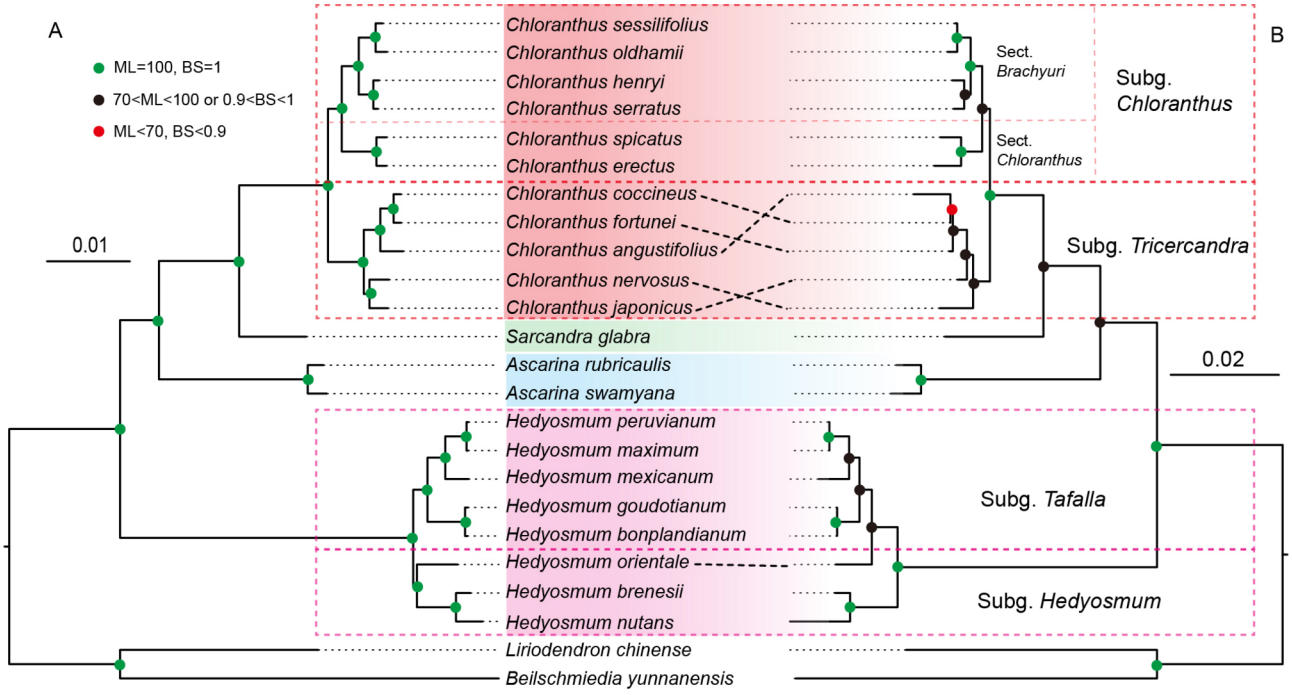

Fig. 5 Phylogram of Chloranthaceae inferred from the plastome (left) and nuclear ribosomal DNA (right) by using the Bayesian method. ML: maximum likelihood; BI: Bayesian inference

H. goudotianum and *H. bonpandianum*. The second clade, comprised *H. nutans and H. brenesii* as sister species, both of which grouped with *H. orientale*.

Compared with the plastome trees, the nrDNA data yielded slightly different topologies (Fig. 5B), mainly within the *Chloranthus* subgenus *Tricercandra*. The nuclear tree showed only moderate-to-low support for some relationships within this subgenus (Fig. S3). Additionally, *Hedyosmum orientale* grouped with the subgenus *Tafalla* in the nuclear tree, contradicting the result of plastome tree and challenging its placement in the subgenus *Hedyosmum* according to the current taxonomic framework.

Biogeographical reconstruction.

The DEC model was considered appropriate and selected for both the extant-only and comprehensive phylogenies (Table S10). According to ancestral range reconstructions performed based on the extant Chloranthaceae phylogeny, this family likely originated in Central America and East Asia simultaneously or solely in East Asia (Fig. 6A). Subsequent dispersal patterns indicated expansion into the South Pacific Islands from East Asia, followed by southwestward migration into the Indian Subcontinent. The extant New World *Hedyosmum* species likely radiated southward from Central America to South America (Fig. 6A).

Ancestral range reconstructions yielded similar biogeographic patterns even after the fossil distribution data were included (Fig. 6B). Chloranthaceae's biogeographic origin remains uncertain, with multiple plausible ancestral ranges including East Asia–Central America, East Asia–Europe, East Asia–North America, and East Asia alone—all within the paleogeographic boundaries of the Laurasia. The ancestral range reconstruction results strongly support a Laurasian origin for the family, with subsequent dispersal to Europe, North America, the South Pacific islands, and the Indian Subcontinent through dispersal events. However, the pathway into Antarctica remains unclear, potentially involving stepping-stone dispersal via the Indian Subcontinent or Africa during periods of conducive paleo-climatic connectivity. For *Hedyosmum* and its stem groups, ancestral reconstructions suggest an origin in either Central America or Europe, with the European hypothesis being reinforced by the occurrence of the earliest fossil representatives (*Hedyflora*) in European deposits (Fig. 6B).

Discussion

Chloroplasts serve as dynamic metabolic hubs playing fundamental roles in sustaining life through photosynthesis, which involves the conversion of solar energy into carbohydrates and release of oxygen [64]. This ability to capture and use sunlight is essential for the survival and productivity of most living organisms. The chloroplast genome encodes crucial proteins involved in photosynthesis and metabolism [65]. Advancements in high-throughput sequencing have markedly accelerated plastome research [66]. Although plastomes from seven

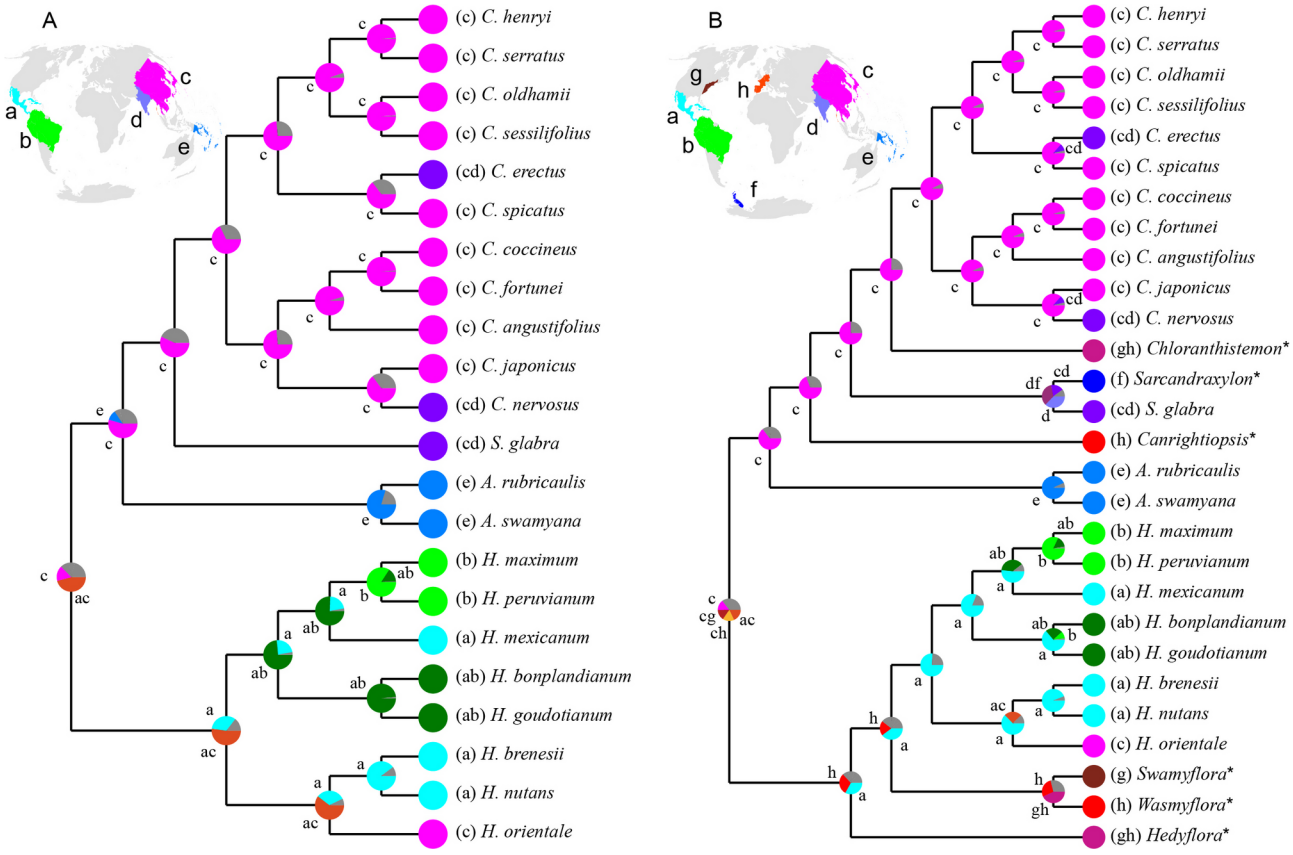

Fig. 6 Ancestral geographical range analysis of Choranthaceae. (**A**) Area reconstructed using the extant Chloranthaceae over the Maximum likelihood tree generated in the present study. (**B**) Area reconstructions integrating extant and fossil Chloranthaceae over a tree obtained from Friis et al.'s study [43]. C., *Chloranthus*; S., *Sarcandra*; A., *Ascarina*; H., *Hedyosmum*. a, Central America; b, South America; c, East Asia; d, Indian Subcontinent; e, South Pacific Islands; f, Antarctica Peninsula; g, Eastern North America; h, Southwest Europe. Asterisks indicate fossil Chloranthaceae. *Hedyflora*, *Wasmyflora*, and *Canrightiopsis* all trace back to Early Cretaceous (Aptian–Albian), *Swamyflora* to Early Cretaceous (Albian), *Sarcandraxylon* to Late Cretaceous (Santonian–Campanian), and *Chloranthistemon* to Mid-Cretaceous (Albian–Cenomanian)

Chloranthaceae species, including six *Chloranthus* and one *Sarcandra* species, have been previously reported [31–38], large-scale comparative analyses are lacking. In this study, we sequenced, assembled, annotated, and compared plastomes from 22 Chloranthaceae species, covering all four genera in this family.

Variations in the plastid genome

Plastomes often exhibit a quadripartite structure in various organisms from photosynthetic algae to seed plants [67]. Consistently, the plastomes of all 22 Chloranthaceae species in this study displayed the typical quadripartite structure (Fig. 1), with genome sizes ranging from 157,449 bp (*C. fortunei*) to 159,218 bp (*H. brenesii*) (Table 1). These variations are consistent with previously reported lengths for Chloranthaceae plastomes, as reported by Zeng et al. [34].

Gene content and arrangement of Chloranthaceae plastomes are consistent across the species; however, the extent of IR regions varies (Figs. 1 and 2; Table 1). Most species contain 130 genes, except for the five *Hedyosmum* species, which were found to contain 131 genes due to differences in IR expansion or contraction (Table 1). Furthermore, the pseudogene $\psi trnH^{GUG}$ at the LSC/IRb junction was missing in *C. angustifolius* due to IR region contraction (Fig. 2). These results are inconsistent with those of other studies, which have reported that *C. japonicus*, *C. henryi*, and *C. fortunei* contain 131 genes [32, 35, 37]. However, in *C. japonicus* [32] and *C. henryi* [35], the pseudogene *ψycf1* was erroneously included in the total gene count. In addition, the annotation of *C. fortunei* by Kang et al. [37], although aligning with the present study results, contains errors in the count of repeat genes in the IR regions. These findings confirm the relatively conserved nature of the Chloranthaceae plastomes, with minor variations mainly attributed to IR expansion or contraction. Compared with the basal angiosperm *Amborella trichopoda* [68], Chloranthaceae plastomes lack two hypothetical genes, *ycf15* and *ycf68*, which locate in the IR regions of many plant species. Both genes are known for their exceptionally low rates of variations. It is believed that their conservation is primarily a result

of their genomic position, rather than specific functions [69, 70].

Three factors contribute to the variations in plastome size [71]: IR region expansion or contraction; gene loss and additional gene duplications outside the IR [72, 73], and differences in the sizes of introns and intergenic spacer regions [74, 75]. Moreover, repeat sequences, such as tandem and dispersed repeats, are known to influence plastome size variations across specific plant lineages [76, 77]. Our findings corroborate the hypothesis that the expansion or contraction of IR regions contributes to plastome size variation in Chloranthaceae, as evidenced by the positive correlation between plastome size and IR length noted in the present study (Fig. 4). However, variations in IR length within Chloranthaceae species were relatively small, ranging from 26,132 bp to 26,508 bp, whereas the total plastome size ranged from 157,449 bp to 159,218 bp (Table 1). The results suggest that the IR length contributes slightly to the overall plastome size variation. Further analyses unveiled that SSRs likely contribute to plastome size variation in Chloranthaceae. While the number of dispersed repeats positively correlated with plastome size, this correlation was non-significant. Moreover, the number of tandem repeats shows little correlation with plastome size in Chloranthaceae (Fig. S2).

The variation in IR regions provides significant implications related to phylogenetic relations within Chloranthaceae. Notably, species within *Hedyosmum* exhibited a pronounced tendency for IR expansion, whereas species from the other three genera demonstrated IR region contraction compared with those from *Hedyosmum*. Among the eight *Hedyosmum* species examined, five species (i.e., *H. bonplandianum*, *H. goudotianum*, *H. orientale*, *H. nutans*, and *H. brenesii*) contained two copies of the *trnH* gene and formed a basal grade in our phylogenetic analysis. In these five species, the IR regions expanded into the LSC as well as the SSC region (Fig. 2). However, in the remaining three *Hedyosmum* species (*H. peruvianum*, *H. maximum*, and *H. mexicanum*), the IR expansion was limited to the SSC region. This may be because the IR region in the common ancestor of Chloranthaceae species is relatively small; however, it probably underwent expansion in the ancestor of *Hedyosmum*, later reverting to its ancestral state and contracting partially in the clade comprising *H. peruvianum*, *H. maximum*, and *H. mexicanum*. Interestingly, while IR expansion is commonly believed to occur more frequently toward the LSC region, rather than the SSC region [78], our results support bidirectional expansion of IR regions in *Hedyosmum*.

Phylogenetic relationships within Chloranthaceae

The advent of next-generation sequencing (NGS) technologies has significantly advanced phylogenetic studies by allowing the use of complete plastome sequences [79–82]. Despite offering significant benefits, the use of chloroplast genome data remains associated with issues such as plastome capture, as chloroplast data primarily represent maternal inheritance [83]. Moreover, despite the increasing accessibility of NGS technology, the high cost of sequencing whole nuclear genomes remains a major barrier to its widespread application, especially in plant families such as Chloranthaceae, which possess relatively large nuclear genomes [19, 23]. Therefore, researchers continue to often rely on nuclear ribosomal ITS regions as a cost-effective alternative for resolving the interspecific and intergeneric relationships between closely related species or genera. Given these considerations, we conducted a comparative analysis of phylogenetic trees constructed from the plastome genes and those based on nrDNA sequences to assess their congruence.

Although the nuclear phylogeny exhibited lower node support for the nuclear tree than for the chloroplast tree due to the limited informative sites in the nrDNA sequences, both nuclear and plastome phylogenies consistently recovered identical intergeneric relationships. This result is consistent with those of previous studies using molecular [9, 1029, 30] or morphological data [84, 85]. The congruence between the nuclear and plastome phylogenies provides a well-supported, robust framework for understanding the evolutionary intergeneric relationships among Chloranthaceae family members. However, plastome data offered greater support in resolving infrageneric relationships than the nrDNA data, particularly within the subgenus *Tricercandra* (Fig. 5). Consequently, the observed discrepancy can be attributed to the limited phylogenetic information in the nrDNA, rather than conflicting evolutionary histories, except for some cases discussed below.

Our plastome dataset-based phylogenetic analyses provided robust resolution of interspecific relationships within the genus *Chloranthus*. Notably, the phylogenetic results of Antonelli and Sanmartín [30] and Lu et al. [86] are slightly inconsistent with our results. Antonelli and Sanmartín [30] reconstructed the phylogeny of *Chloranthus* by using only two plastid genes (*rbcL* and *rps16*) and nrDNA ITS sequences, resulting in low node support and uncertain relationships. Therefore, the grade consisting of *C. nervosus*, *C. holostegius*, and *C. japonicus* in Antonelli and Sanmartín [30] is questionable. Notably, Kong [87] have suggested synonymizing *C. holostegius* with *C. nervosus*. This taxonomic treatment has been further supported by the results of a recent molecular study by Kang and Yoo [88]. Similarly, Lu et al. [86] constructed a *Chloranthus* phylogeny based on four concatenated plastid genes (*rbcL*, *rpl20-rps12*, *rps16*, and *trnL-F*), but their results showed only moderate support for key clades. For example, *C. nervosus* clustered with a pair of

sister species (*C. angustifolius* and *C. fortunei*), while *C. japonicus* was positioned as a successive sister lineage. However, this relationship lacked statistical robustness, raising doubts about its accuracy. Kong et al. [8] described the taxonomic implications of the *Chloranthus* phylogeny for traditional taxonomic proposals, which culminated in a more natural infrageneric classification system proposed by Kong [87]. According to this system, *Chloranthus* is divided into two subgenera: *Chloranthus* and *Tricercandra*. Additionally, the subgenus *Chloranthus* is subdivided into two sections: sect. *Chloranthus* and sect. *Brachyuri* (Fig. 5).

Hedyosmum is the largest genus within the Chloranthaceae family, comprising the subgenera *Hedyosmum* and *Tafalla* [89]. Antonelli and Sanmartín [30] and Zhang et al. [9] have attempted to resolve the phylogenetic relationships within this genus. However, the attempts remained unsuccessful due to limited number of molecular markers. Additionally, there has been considerable disagreement regarding the systematic placement of *H. orientale*, the only species distributed in Asia. Antonelli and Sanmartín [30] suggested *H. orientale* is a sister to the subgenus *Tafalla*, whereas Zhang et al. [9] proposed that *H. orientale* is a sister to all the remaining species in *Hedyosmum* [9]. In our study, *H. orientale* occupied a basal position within the subgenus *Tafalla* in the nuclear phylogenetic tree (Fig. 5), consistent with the findings of Antonelli and Sanmartín [30]. However, in the chloroplast tree, *H. orientale* formed a strongly supported cluster with two members of the subgenus *Hedyosmum* (*H. brenesii* and *H. nutans*). Previous phylogenetic research using chloroplast regions suggested that *H. orientale* was sister to all other species of *Hedyosmum* with high support and this relationship was coincided with the occurrence of InDels [10]. While InDels are generally considered less common and less prone to reversal than simple sequence substitutions [90, 91], some recent studies have reported a high level of homoplasy (multiple independent origins) in InDels [92]. Therefore, the two shared InDels supported the separation of *H. orientale* from other *Hedyosmum* species in Zhang et al.'s study [10] may have resulted from homoplastic evolution. Considering that both chloroplast and nuclear phylogenies strongly support the systematic position of *H. orientale*, we hypothesize that *H. orientale* may have captured the plastomes of *H. brenesii* and *H. nutans* through ancient hybridization with their common ancestor.

Biogeographical and taxonomic implications

Understanding the drivers of intercontinental disjunctions in plant lineages remains a pivotal challenge in historical biogeography [39, 93]. Chloranthaceae is a classic example of an amphi-Pacific disjunction, with extant species primarily distributed across the Neotropics and tropical to temperate East Asia. This distribution has traditionally been attributed to either vicariance resulting from continental drift (e.g., Gondwanan fragmentation) or long-distance dispersal across oceanic barriers [94]. In our study, the biogeographic analyses reconstructed East Asia (either alone or in combination with other Laurasian regions) as the most likely ancestral area for the family. This result strongly supports the Laurasian origin hypothesis, consistent with the hypothesis proposed by Raven and Axelrod [39].

Fossil evidence of Chloranthaceae dating back to the mid–Late Cretaceous (Aptian–Campanian; ~120–70 Ma), a period characterized by significantly warmer global temperatures than modern conditions [95], further supports a Laurasian origin. Notably, the Cretaceous fossil record indicates a Laurasian origin, with most specimens occurring in eastern North America and western Europe, while *Sarcandraxylon*, discovered in Antarctica, suggested the sole Gondwanan presence. The extant Chloranthaceae exhibited a pantropical distribution, with only a few *Chloranthus* species expanding into temperate East Asia. This paleobiogeographic dichotomy offers a robust support for the Laurasian origin hypothesis for Chloranthaceae, coinciding with peak greenhouse conditions and persistent Laurasian–Gondwanan continental connectivity. Under this model, early chloranthoids likely achieved global distributions by exploiting the Cretaceous Thermal Maximum, as evident in the cosmopolitan *Asteropollis*-type pollen record [43]. During Upper-Cretaceous, reduced latitudinal temperature gradients facilitated trans-equatorial migrations. The Antarctic *Sarcandraxylon* fossils may represent southward dispersal events during this period. Subsequent Paleogene cooling induced thermophilic range contraction, forcing surviving lineages into tropical refuge while eliminating mid-latitude populations, thereby leading to the intercontinental disjunctions persisting to date. A similar pattern has been observed in Symplocaceae [93] and Urticaceae [96]. *Chloranthus* distribution in temperate regions potentially indicates initial range contraction to tropical zones during climatic cooling, followed by secondary dispersal from tropical refugia following post-glacial warming, which might have contributed to its extant subtropical-temperate distribution.

For *Hedyosmum*, ancestral reconstructions proposed two plausible scenarios: (1) a Laurasian origin (spanning Asia and Central America) followed by regional extinctions, leaving *H. orientale* as a relict Asian lineage disjunct from its neotropical congeners, or (2) a Central American origin, with *H. orientale* representing a transoceanic dispersal event (via long-distance dispersal or hypothetical land bridges). The first scenario is supported by the fossil records of *Hedyflora*, *Swamyflora*, and *Wasmyflora* in North America and Eourpe. While

the second scenario appears biogeographically unlikely at first glance, it cannot be entirely ruled out. Notably, the fruits of *Hedyosmum* are succulent and turn white or purple at maturity, traits that may attract avian dispersers [89]. Direct trans-Pacific long-distance dispersal between Asia and the Americas has been documented or inferred in other plant families such as Ericaceae [97] and Lardizabalaceae [98]. Furthermore, Shaffer et al. [99] reported that the sooty shearwater (*Ardenna grisea*, Procellariidae), a small seabird, is capable of trans-Pacific flights. Thus, *Hedyosmum* species could have dispersed from Central America to East Asia through either direct long-distance dispersal or a stepping-stone migration pattern facilitated by birds.

The phylogenetic results for *Hedyosmum* present notable taxonomic implications. The chloroplast tree supports the monophyly of the subgenus *Tafalla* aligning with the traditional infrageneric classification (Fig. 5). By contrast, the nuclear tree indicates paraphyly within this subgenus. However, in the present study, sampling of species was limited, and we excluded three *Hedyosmum* species, namely, *H. arborescens*, *H. neblinae*, and *H. gentryi*, reported to contribute to the polyphyly of the subgenus *Tafalla* according to Zhang et al. [10]. Moreover, the phylogenetic framework derived from nrDNA is not robust. Therefore, more extensive sampling, along with a phylogenomic analysis conducted using more nuclear genes, is required to establish a solid taxonomic framework.

Conclusions

In this study, using Illumina sequencing data, we sequenced, assembled, annotated, and compared the plastomes from 22 species representing all genera of Chloranthaceae. To our knowledge, this study is the first to examine plastome variation patterns and their phylogenetic implications within chloranthoid species. Our results revealed their tetrad structures and shared characteristics with other angiosperms. Moreover, the species showed a high degree of conservation in the sequence length, genome structure, gene content, and gene order. Slight IR expansion was observed within the basal grade of *Hedyosmum*, exhibiting significant phylogenetic patterns. However, subtle variations in plastome size were found, primarily ascribed to changes in the IR region and the number of SSRs. Additionally, phylogenetic analyses conducted using both plastome and nrDNA data suggested that *H. orientale*, the only *Hedyosmum* species distributed in tropical Asia, is embedded within *Hedyosmum*, rather than being a sister to all neotropical *Hedyosmum* species. This inconsistent placement of *H. orientale* in the plastome and nuclear tree suggests the occurrence of hybridization events among closely related species. Finally, this study provides evidence for the origin of Chloranthaceae species in Laurasia, with boreotropical vicariance most plausibly explaining their current distribution pattern.

Abbreviations

BI	Bayesian inference
CDS	Coding regions
CTAB	Cetyltrimethylammonium bromide
DEC	Divergence-extinction-cladogenesis
IGS	Intergenic regions
IR	Inverted repeat
LSC	Large single copy
ML	Maximum likelihood
NGS	Next-generation sequencing
nrDNA	Nuclear ribosomal DNA
PCG	Protein-coding gene
SSR	Simple sequence repeat

Supplementary Information

The online version contains supplementary material available at https://doi.org/10.1186/s12870-025-06586-8.

Supplementary Material 1

Supplementary Material 2

Acknowledgements

We would like to express our gratitude to Taylor S. Feild for providing samples of Hedyosmum and Ascarina species, and Wei-Bin Xu, Bo Pan, Zhao-Cen Lu, Yu-Liang Jiang, Xin-Lei Zhao, and Jia-Hui Li for collecting samples of Chloranthus and Hedyosmum. We express our gratitude to the editor and two anonymous reviewers for the valuable suggestions and kind comments.

Author contributions

PWL and QZ conceived the study. QZ, YBL, and XMQ conducted the field work. YBL conducted the experiments. PWL analyzed the data, and wrote the manuscript. All the authors read and approved the manuscript.

Funding

This research was financially supported by the Natural Science Foundation of Guangxi Zhuang Autonomous Region (2025GXNSFAA069328, 2025GXNSFAA069230, 2021GXNSFAA196049), National Natural Science Foundation of China (31200174), Fundamental Research Fund of Guangxi Institute of Botany (GZY23002) and the Fund of Guangxi Key Laboratory of Plant Conservation and Restoration Ecology in Karst Terrain (No.22-035-26).

Data availability

The datasets supporting the conclusions of this article are included within the article and the supplementary files. We deposited sequencing data in the Sequence Read Archive (SRA), National Center for Biotechnology Information (NCBI), BioProject ID: PRJNA1205889. The annotated chloroplast genomes and nuclear ribosomal DNA sequences reported in present study were deposited in NCBI with accession numbers PQ728875–PQ728896 and PQ805146–PQ805167, respectively (Table S1).

Declarations

Ethics approval and consent to participate

All plant samples used in the study were collected from natural habitats and none of them were listed as nationally key protected plant species. According to national and local legislation, no specific permission was required for collecting these plants. Specimens of *Ascarina* and *Hedyosmum* (excluding *H. orientale*) were authenticated by Taylor S. Feild, while the remaining samples were identified by Qiang Zhang. Voucher specimens have been deposited in the Herbarium of Guangxi Institute of Botany, Chinese Academy of Sciences (IBK).

Consent for publication

Not applicable.

Competing interests
The authors declare no competing interests.

Author details
[1]Guangxi Key Laboratory of Plant Conservation and Restoration Ecology in Karst Terrain, Guangxi Institute of Botany, Guangxi Zhuang Autonomous Region and Chinese Academy of Sciences, Guilin 541006, China

Received: 25 December 2024 / Accepted: 18 April 2025
Published online: 25 April 2025

References

1. Todzia CA. Chloranthaceae. In: The Families and Genera of Vascular Plants Flowering Plants, Dicotyledons: Magnoliid, Hamamelid and Caryophyllid Families. Edited by Kubitzki K, Rohwer JG, Bittrich V, vol. 2. Berlin & Heidelberg: Springer-Verlag; 1993: 281–287.
2. Qiu YL, Lee JH, Bernasconi-Quadroni F, Soltis DE, Soltis PS, Zanis M, et al. The earliest angiosperms: evidence from mitochondrial, plastid and nuclear genomes. Nature. 1999;402(6760):404–7.
3. Eklund H, Doyle JA, Herendeen PS. Morphological phylogenetic analysis of living and fossil Chloranthaceae. Int J Plant Sci. 2004;165(1):107–51.
4. Endress PK. Reproductive structures and phylogenetic significance of extant primitive angiosperms. Plant Syst Evol. 1986;152(1–2):1–28.
5. Carlquist S. Presence of vessels in wood of *Sarcandra* (Chloranthaceae); comments on vessel origins in angiosperms. Am J Bot. 1987;74(12):1765–71.
6. Crane PR, Friis EM, Pedersen KR. Reproductive structure and function in cretaceous Chloranthaceae. Plant Syst Evol. 1989;165(3–4):211–26.
7. Eklund H, Friis EM, Pedersen KR. Chloranthaceous floral structures from the late cretaceous of Sweden. Plant Syst Evol. 1997;207(1–2):13–42.
8. Kong HZ, Chen ZD, Lu AM. Phylogeny of *Chloranthus* (Chloranthaceae) based on nuclear ribosomal ITS and plastid *trnL-F* sequence data. Am J Bot. 2002;89(6):940–6.
9. Zhang Q, Antonelli A, Feild TS, Kong HZ. Revisiting taxonomy, morphological evolution, and fossil calibration strategies in Chloranthaceae. J Syst Evol. 2011;49(4):315–29.
10. Zhang Q, Feild TS, Antonelli A. Assessing the impact of phylogenetic incongruence on taxonomy, floral evolution, biogeographical history, and phylogenetic diversity. Am J Bot. 2015;102(4):566–80.
11. Endress PK, Doyle JA. Ancestral traits and specializations in the flowers of the basal grade of living angiosperms. Taxon. 2015;64(6):1093–116.
12. Friis EM, Crane PR, Pedersen KR. *Hedyosmum*-like fossils in the early cretaceous diversification of angiosperms. Int J Plant Sci. 2019;180(3):232–9.
13. Cao CM, Peng Y, Shi QW, Xiao PG. Chemical constituents and bioactivities of plants of Chloranthaceae. Chem Biodivers. 2008;5(2):219–38.
14. Li CJ, Zhang DM, Luo YM, Yu SS, Li Y, Lu Y. Bis-sesquiterpenes and diterpenes from *Chloranthus henryi*. Phytochemistry. 2008;69(16):2867–74.
15. Tolardo R, Zetterman L, Bitencourtt DR, Mora TC, de Oliveira FL, Biavatti MW, et al. Evaluation of behavioral and Pharmacological effects of *Hedyosmum Brasiliense* and isolated sesquiterpene lactones in rodents. J Ethnopharmacol. 2010;128(1):63–70.
16. Zhang ML, Liu D, Fan GQ, Wang RX, Lu XH, Gu YC, et al. Constituents from Chloranthaceae plants and their biological activities. Heterocycl Commun. 2016;22(4):175–220.
17. Radice M, Tasambay A, Perez A, Dieguez-Santana K, Sacchetti G, Buso P, et al. Ethnopharmacology, phytochemistry and Pharmacology of the genus *Hedyosmum* (Chloranthaceae): A review. J Ethnopharmacol. 2019;244:111932.
18. Liu YY, Li YZ, Huang SQ, Zhang HW, Deng C, Song XM, et al. Genus *Chloranthus*: A comprehensive review of its phytochemistry, pharmacology, and uses. Arab J Chem. 2022;15(11):104260.
19. Guo X, Fang DM, Sahu SK, Yang S, Guang XM, Folk R, et al. *Chloranthus* genome provides insights into the early diversification of angiosperms. Nat Commun. 2021;12(1):6930.
20. Yang YZ, Sun PC, Lv LK, Wang DL, Ru DF, Li Y, et al. Prickly waterlily and rigid hornwort genomes shed light on early angiosperm evolution. Nat Plants. 2020;6(3):215–22.
21. Zhang LS, Chen F, Zhang XT, Li Z, Zhao YY, Lohaus R, et al. The water Lily genome and the early evolution of flowering plants. Nature. 2020;577(7788):79–84.
22. Leebens-Mack JH, Barker MS, Carpenter EJ, Deyholos MK, Gitzendanner MA, Graham SW, et al. One thousand plant transcriptomes and the phylogenomics of green plants. Nature. 2019;574(7780):679–85.
23. Ma JX, Sun PC, Wang DD, Wang ZY, Yang J, Li Y, et al. The *Chloranthus sessilifolius* genome provides insight into early diversification of angiosperms. Nat Commun. 2021;12(1):6929.
24. Zeng LP, Zhang Q, Sun RR, Kong HZ, Zhang N, Ma H. Resolution of deep angiosperm phylogeny using conserved nuclear genes and estimates of early divergence times. Nat Commun. 2014;5:4956.
25. Zuntini AR, Carruthers T, Maurin O, Bailey PC, Leempoel K, Brewer GE, et al. Phylogenomics and the rise of the angiosperms. Nature. 2024;629(8011):843–54.
26. Li HT, Yi TS, Gao LM, Ma PF, Zhang T, Yang JB, et al. Origin of angiosperms and the puzzle of the jurassic gap. Nat Plants. 2019;5(5):461–70.
27. Qiu YL, Lee J, Bernasconi-Quadroni F, Soltis DE, Soltis PS, Zanis M, et al. Phylogeny of basal angiosperms: analyses of five genes from three genomes. Int J Plant Sci. 2000;161(6):S3–27.
28. Zanis MJ, Soltis DE, Soltis PS, Mathews S, Donoghue MJ. The root of the angiosperms revisited. Proc Natl Acad Sci USA. 2002;99(10):6848–53.
29. Zhang LB, Renner S. The deepest splits in Chloranthaceae as resolved by Chloroplast sequences. Int J Plant Sci. 2003;164(5):S383–92.
30. Antonelli A, Sanmartín I. Mass extinction, gradual cooling, or rapid radiation? Reconstructing the Spatiotemporal evolution of the ancient angiosperm genus *Hedyosmum* (Chloranthaceae) using empirical and simulated approaches. Syst Biol. 2011;60(5):596–615.
31. Hansen DR, Dastidar SG, Cai ZQ, Penaflor C, Kuehl JV, Boore JL, et al. Phylogenetic and evolutionary implications of complete Chloroplast genome sequences of four early-diverging angiosperms: *Buxus* (Buxaceae), *Chloranthus* (Chloranthaceae), *Dioscorea* (Dioscoreaceae), and *Illicium* (Schisandraceae). Mol Phylogenet Evol. 2007;45(2):547–63.
32. Sun J, Zhang G, Li YM, Chen Y, Zhang XF, Tang ZS, et al. The complete Chloroplast genome sequence of *Chloranthus japonicus*. Mitochondrial DNA Part A. 2016;27(5):3202–4.
33. Han EK, Cho WB, Choi G, Lee JH. The complete Chloroplast genome of *Sarcandra glabra* (Chloranthaceae): A perianthless basal angiosperm. Mitochondrial DNA B Resour. 2018;3(2):661–2.
34. Zeng CX, Hollingsworth PM, Yang J, He ZS, Zhang ZR, Li DZ, et al. Genome skimming herbarium specimens for DNA barcoding and phylogenomics. Plant Methods. 2018;14:43.
35. Liu XD, Liao XY, Liu ZJ, Lan SR. Complete Chloroplast genome of *Chloranthus henryi* (Chloranthaceae). Mitochondrial DNA B Resour. 2019;4(2):2964–5.
36. Liao XY, Liu XD, Jiang YT, Zhou Z, Xu XY, Zheng Y, et al. The complete Chloroplast genome of medicine and horticultural plant *Chloranthus spicatus* (Chloranthaceae). Mitochondrial DNA B Resour. 2020;5(2):1293–4.
37. Kang JS, Kim BY, Yoo KO. The complete plastid genome sequence of *Chloranthus Fortunei* (A. Gray) Solms-Laub. In Chloranthaceae. Mitochondrial DNA B Resour. 2022;7(10):1829–33.
38. Yao S-T, Lu Y-B, Zhang Z-J, Li C, Wang P-F, Qin X-M. The complete Chloroplast genome of *Chloranthus nervosus* Collett ex Hemsl. 1890 (Chloranthaceae). Mitochondrial DNA B Resour. 2023;8(11):1224–8.
39. Raven PH, Axelrod DI. Biogeography and past continental movements. Ann Mo Bot Gard. 1974;61(3):539–673.
40. Krutzsch W. Paleogeography and historical phytogeography (paleochorology) in the neophyticum. Plant Syst Evol. 1989;162(1):5–61.
41. Zhou Z-K. Origin, systematics and distribution of Chloranthaceae. Acta Bot Yunnan. 1993;15(4):321–321.
42. Chen HS, Cheng YQ. The origin, differentiation and geography of Chloranthaceae. J Trop Subtrop Bot. 1994;2(4):31–44.
43. Friis EM, Crane PR, Pedersen KR, Marone F. Cretaceous chloranthoids: early prominence, extinct diversity and missing links. Ann Bot. 2024;133(2):225–60.
44. Lu YB, Jiang YL, Qin XM, Zhang Q. Morphological diversity and geographical distribution of *Chloranthus* in China. Guihaia. 2020;40(1):31–43.
45. Doyle JJ, Doyle JL. A rapid DNA isolation procedure for small quantities of fresh leaf tissue. Phytochem Bull. 1987;19(1):11–5.
46. Bolger AM, Lohse M, Usadel B, Trimmomatic. A flexible trimmer for illumina sequence data. Bioinformatics. 2014;30(15):2114–20.
47. Jin JJ, Yu WB, Yang JB, Song Y, dePamphilis CW, Yi TS, et al. GetOrganelle: A fast and versatile toolkit for accurate de Novo assembly of organelle genomes. Genome Biol. 2020;21(1):241.
48. Kearse M, Moir R, Wilson A, Stones-Havas S, Cheung M, Sturrock S, et al. Geneious basic: an integrated and extendable desktop software platform

for the organization and analysis of sequence data. Bioinformatics. 2012;28(12):1647–9.
49. Qu XJ, Moore MJ, Li DZ, Yi TS. PGA: A software package for rapid, accurate, and flexible batch annotation of plastomes. Plant Methods. 2019;15:50.
50. Schattner P, Brooks AN, Lowe TM. The tRNAscan-SE, Snoscan and SnoGPS web servers for the detection of tRNAs and snornas. Nucleic Acids Res. 2005;33:W686–9.
51. Greiner S, Lehwark P, Bock R. OrganellarGenomeDRAW (OGDRAW) version 1.3.1: expanded toolkit for the graphical visualization of organellar genomes. Nucleic Acids Res. 2019;47(W1):W59–64.
52. Beier S, Thiel T, Munch T, Scholz U, Mascher M. MISA-web: A web server for microsatellite prediction. Bioinformatics. 2017;33(16):2583–5.
53. Kurtz S, Choudhuri JV, Ohlebusch E, Schleiermacher C, Stoye J, Giegerich R, REPuter. The manifold applications of repeat analysis on a genomic scale. Nucleic Acids Res. 2001;29(22):4633–42.
54. Benson G. Tandem repeats finder: A program to analyze DNA sequences. Nucleic Acids Res. 1999;27(2):573–80.
55. R Core Team. R: A Language and environment for statistical computing team. Vienna: R Core Team; 2024.
56. Miller MA, Pfeiffer W, Schwartz T. Creating the CIPRES Science Gateway for inference of large phylogenetic trees. In: Proceedings of the Gateway Computing Environments Workshop (GCE): 2010; New Orlens, LA.: Ieee: 1–8.
57. Kalyaanamoorthy S, Minh BQ, Wong TKF, von Haeseler A, Jermiin LS. ModelFinder: fast model selection for accurate phylogenetic estimates. Nat Methods. 2017;14(6):587–9.
58. Nguyen L-T, Schmidt HA, von Haeseler A, Minh BQ. IQ-TREE: A fast and effective stochastic algorithm for estimating maximum-likelihood phylogenies. Mol Biol Evol. 2015;32(1):268–74.
59. 5Stamatakis A. RAxML version 8: A tool for phylogenetic analysis and post-analysis of large phylogenies. Bioinformatics. 2014;30(9):1312–3.
60. Ronquist F, Huelsenbeck JP. MrBayes 3: bayesian phylogenetic inference under mixed models. Bioinformatics. 2003;19(12):1572–4.
61. Walker JW, Walker AG. Ultrastructure of lower cretaceous angiosperm pollen and the origin and early evolution of flowering plants. Ann Mo Bot Gard. 1984;71(2):464–521.
62. Matzke NJ. Probabilistic historical biogeography: new models for founder-event speciation, imperfect detection, and fossils allow improved accuracy and model-testing. Front Biogeogr. 2013;5(4):242–8.
63. Yu Y, Blair C, He X. RASP 4: ancestral state reconstruction tool for multiple genes and characters. Mol Biol Evol. 2020;37(2):604–6.
64. Bock R. Structure, function, and inheritance of plastid genomes. In: Cell and Molecular Biology of Plastids. Edited by Bock R. Berlin, Heidelberg: Springer Berlin Heidelberg; 2007: 29–63.
65. Daniell H, Lin CS, Yu M, Chang WJ. Chloroplast genomes: diversity, evolution, and applications in genetic engineering. Genome Biol. 2016;17:134.
66. Wu P, Chen H, Xu C, Yang J, Zhang XC, Zhou SL. NOVOWrap: an automated solution for plastid genome assembly and structure standardization. Mol Ecol Resour. 2021;21(6):2177–86.
67. Kwon EC, Kim JH, Kim NS. Comprehensive genomic analyses with 115 plastomes from algae to seed plants: structure, gene contents, GC contents, and introns. Genes Genom. 2020;42(5):553–70.
68. Goremykin VV, Hirsch-Ernst KI, Wolfl S, Hellwig FH. Analysis of the *Amborella trichopoda* Chloroplast genome sequence suggests that *Amborella* is not a basal angiosperm. Mol Biol Evol. 2003;20(9):1499–505.
69. Perry AS, Wolfe KH. Nucleotide substitution rates in legume Chloroplast DNA depend on the presence of the inverted repeat. J Mol Evol. 2002;55(5):501–8.
70. Raubeson LA, Peery R, Chumley TW, Dziubek C, Fourcade HM, Boore JL, et al. Comparative Chloroplast genomics: analyses including new sequences from the angiosperms *Nuphar advena* and R*anunculus macranthus*. BMC Genomics. 2007;8:174.
71. Jansen RK, Ruhlman TA. Plastid Genomes of Seed Plants. In: Genomics of Chloroplasts and Mitochondria. Edited by Bock R, Knoop V. New York & London: Springer Dordrecht Heidelberg; 2012: 103–120.
72. Wolfe KH, Morden CW, Palmer JD. Function and evolution of a minimal plastid genome from a nonphotosynthetic parasitic plant. Proc Natl Acad Sci USA. 1992;89(22):10648–52.
73. Wakasugi T, Tsudzuki J, Ito S, Nakashima K, Tsudzuki T, Sugiura M. Loss of all Ndh genes as determined by sequencing the entire Chloroplast genome of the black pine *Pinus thunbergii*. Proc Natl Acad Sci USA. 1994;91(21):9794–8.
74. Masood MS, Nishikawa T, Fukuoka S, Njenga PK, Tsudzuki T, Kadowaki K. The complete nucleotide sequence of wild rice (*Oryza nivara*) Chloroplast genome: first genome wide comparative sequence analysis of wild and cultivated rice. Gene. 2004;340(1):133–9.
75. Greiner S, Wang X, Rauwolf U, Silber MV, Mayer K, Meurer J, et al. The complete nucleotide sequences of the five genetically distinct plastid genomes of *Oenothera*, subsection *Oenothera*: I. Sequence evaluation and plastome evolution. Nucleic Acids Res. 2008;36(7):2366–78.
76. Dugas DV, Hernandez D, Koenen EJM, Schwarz E, Straub S, Hughes CE, et al. Mimosoid legume plastome evolution: IR expansion, tandem repeat expansions, and accelerated rate of evolution in *ClpP*. Sci Rep. 2015;5:16958.
77. Wang YH, Qu XJ, Chen SY, Li DZ, Yi TS. Plastomes of mimosoideae: structural and size variation, sequence divergence, and phylogenetic implication. Tree Genet Genom. 2017;13(2):41.
78. Rabah SO, Shrestha B, Hajrah NH, Sabir MJ, Alharby HF, Sabir MJ, et al. *Passiflora* plastome sequencing reveals widespread genomic rearrangements. J Syst Evol. 2019;57(1):1–14.
79. Yang JB, Tang M, Li HT, Zhang ZR, Li DZ. Complete Chloroplast genome of the genus *Cymbidium*: lights into the species identification, phylogenetic implications and population genetic analyses. BMC Evol Biol. 2013;13:84.
80. Feng YL, Wicke S, Li JW, Han Y, Lin CS, Li DZ, et al. Lineage-specific reductions of plastid genomes in an Orchid tribe with partially and fully mycoheterotrophic species. Genome Biol Evol. 2016;8(7):2164–75.
81. Amenu SG, Wei N, Wu L, Oyebanji O, Hu GW, Zhou YD, et al. Phylogenomic and comparative analyses of coffeeae alliance (Rubiaceae): deep insights into phylogenetic relationships and plastome evolution. BMC Plant Biol. 2022;22(1):88.
82. Yang LH, Shi XZ, Wen F, Kang M. Phylogenomics reveals widespread hybridization and polyploidization in *Henckelia* (Gesneriaceae). Ann Bot. 2023;131(6):953–66.
83. Kim YK, Jo S, Choon SH, Joo MJ, Hong JR, Kwak M, et al. Plastome evolution and phylogeny of orchidaceae, with 24 new sequences. Front Plant Sci. 2020;11:22.
84. Doyle JA, Endress PK. Integrating early cretaceous fossils into the phylogeny of living angiosperms: ANITA lines and relatives of Chloranthaceae. Int J Plant Sci. 2014;175(5):555–600.
85. Doyle JA, Endress PK. Phylogenetic analyses of cretaceous fossils related to Chloranthaceae and their evolutionary implications. Bot Rev. 2018;84(2):156–202.
86. Lu YB, Huang ZP, Qin XM, Zhang Q. Combination of *Chloranthus flavus* into *C. nervosus* based on morphological and molecular evidence. Phytotaxa. 2022;564(2):230–8.
87. Kong HZ. Systematics of the Genus *Chloranthus* Swartz (Chloranthaceae). dissertation. Beijing: Institute of Botany, the Chinese Academy of Sciences; 2000.
88. Kang J-S, Yoo K-O. Taxonomic and phylogenetic study of the subgenus *Tricercandra* in the genus *Chloranthus* (Chloranthaceae). Korean J Plant Taxon. 2023;53(4):243–56.
89. Todzia CA, Chloranthaceae. Hedyosmum. Volume 48. New York: The New York Botanical Garden; 1988.
90. Lloyd DG, Calder VL. Multi-residue gaps, a class of molecular characters with exceptional reliability for phylogenetic analyses. J Evol Biol. 1991;4(1):9–21.
91. Rokas A, Holland PWH. Rave genomic changes as a tool for phylogenetics. Trends Ecol Evol. 2000;15(11):454–9.
92. Ajawatanawong P, Baldauf SL. Evolution of protein indels in plants, animals and fungi. BMC Evol Biol. 2013;13:140.
93. Fritsch PW, Manchester SR, Stone RD, Cruz BC, Almeda F. Northern hemisphere origins of the amphi-Pacific tropical plant family Symplocaceae. J Biogeogr. 2015;42(5):891–901.
94. Givnish TJ, Renner SS. Tropical intercontinental disjunctions: Gondwana breakup, immigration from the boreotropics, and transoceanic dispersal. Int J Plant Sci. 2004;165(4):S1–6.
95. Wu SD, Peng HW, Lian L, Ortiz RD, Erst AS, Jabbour F, et al. Eurasian drylands are both evolutionary cradles and museums of Nitrariaceae diversity. J Biogeogr. 2024;51(8):1387–99.
96. Huang X, Deng T, Moore MJ, Wang H, Li Z, Lin N, et al. Tropical Asian origin, Boreotropical migration and long-distance dispersal in nettles (Urticeae, Urticaceae). Mol Phylogenet Evol. 2019;137:190–9.
97. Lu L, Fritsch PW, Matzke NJ, Wang H, Kron KA, Li DZ, et al. Why is fruit colour so variable? Phylogenetic analyses reveal relationships between fruit-colour evolution, biogeography and diversification. Global Ecol Biogeogr. 2019;28(7):891–903.
98. Wang W, Xiang XG, Xiang KL, Ortiz RC, Jabbour F, Chen ZD. A dated phylogeny of Lardizabalaceae reveals an unusual long-distance dispersal across

the Pacific ocean and the rapid rise of East Asian subtropical evergreen broadleaved forests in the late miocene. Cladistics. 2020;36(5):447–57.
99. Shaffer SA, Tremblay Y, Weimerskirch H, Scott D, Thompson DR, Sagar PM, et al. Migratory shearwaters integrate oceanic resources across the Pacific ocean in an endless summer. Proc Natl Acad Sci USA. 2006;103(34):12799–802.

Publisher's note